ELSEVIER

Journal of Chromatography A, 968 (2002) 89–100

JOURNAL OF CHROMATOGRAPHY A

www.elsevier.com/locate/chroma

Simultaneous microanalysis of *N*-linked oligosaccharides in a glycoprotein using microbore graphitized carbon column liquid chromatography–mass spectrometry

Satsuki Itoh, Nana Kawasaki*, Miyako Ohta, Masashi Hyuga, Sumiko Hyuga, Takao Hayakawa

Division of Biological Chemistry and Biologicals, National Institute of Health Science, 1-18-1, Kamiyoga, Setagaya-ku, Tokyo 158-8501, Japan

Received 25 January 2002; received in revised form 13 June 2002; accepted 19 June 2002

Abstract

We previously reported that graphitized carbon column liquid chromatography–mass spectrometry (GCC-LC–MS) is very useful for the structural analysis of carbohydrates in a glycoprotein. In this study, GCC-LC–MS was adapted for the simultaneous microanalysis of oligosaccharides. A variety of oligosaccharide alditols prepared from fetuin, ribonuclease B, and recombinant human erythropoietin were used as model oligosaccharides. The use of microbore GCC-LC–MS was found to be successful for rapid, sensitive, and simultaneous analysis of high-mannose-type, desialylated fucosyl complex-type, sialylated complex-type, and sialylated fucosyl complex-type oligosaccharide alditols. Furthermore, we demonstrate that this method is applicable to the analysis of carbohydrate heterogeneity in a glycoprotein that possesses diverse oligosaccharides. Microbore GCC-LC–MS was able to characterize high-mannose-type, hybrid-type, and complex-type oligosaccharides in tissue plasminogen activator produced from human melanoma cells in a single analysis.

Keywords: Porous graphitized carbon; Oligosaccharides; Glycoproteins; Proteins

1. Introduction

Glycosylation plays an important role in the biological and biophysical properties of many glycoproteins, including biological activity, antigenicity, metabolic fate, stability, and solubility [1]. The structure of oligosaccharides attached to a glycoprotein is also associated with various developmental stages and pathological states. Therefore, it is necessary to elucidate carbohydrate structure and carbohydrate distribution in a glycoprotein in order to understand the roles of oligosaccharides. Many methods for the structural analysis of oligosaccharides have been developed. High-performance liquid chromatography (HPLC), for example, is effective for the separation of diverse oligosaccharides. The oligosaccharides fractionated by HPLC are characterized by additional types of analysis such as nuclear magnetic resonance (NMR) and MS. When only a very small amount of glycoprotein is available,

*Corresponding author. Tel.: +81-3-3700-1141; fax: +81-3-3707-6950.

E-mail address: nana@nihs.go.jp (N. Kawasaki).

0021-9673/02/$ – see front matter
PII: S0021-9673(02)00951-2

oligosaccharides are derivatized with fluorescence reagents such as 2-aminobenzoic acid (2-AB) and 2-aminopyridine (2-AP) for improvement of detection [2–4]. The structure of the derivatized oligosaccharides can be determined by exoglycosidase treatments and a comparison of the oligosaccharides' retention times with those of standards on reversed-phase, size-fractionation, and normal-phase columns. However, derivatization and purification of the derivatives are time consuming, and the standards are often unavailable.

In a previous study, we demonstrated that liquid chromatography–mass spectrometry (LC–MS) equipped with a graphitized carbon column (GCC) is useful for the structural analysis of *N*-linked (or asparagine-linked) oligosaccharides in glycoproteins. By use of GCC-LC–MS, many different oligosaccharides can be separated well and characterized directly. Previously, high-mannose-type oligosaccharides in ribonuclease B (RNase B) and sialylated fucosyl complex-type oligosaccharides attached to recombinant human erythropoietin (rhEPO) were analyzed by GCC-LC–MS under individual analytical conditions [5,6]. In a biological system, there are a number of glycoproteins that have diverse oligosaccharides, including high-mannose-type, complex-type and hybrid-type, at their multiple glycosylation sites. Therefore, a method by which a variety of oligosaccharides could be analyzed in a single analysis would be extremely useful for determining the structure of glycoproteins. GCC-LC–MS would be especially useful if it were able to analyze the structure of various oligosaccharides in a glycoprotein in a single analysis. Use of a microbore column makes it possible to analyze a small amount of sample rapidly. In addition, use of a microbore column is expected to allow for separation a variety of oligosaccharides by a wide range of gradients.

In this study, we examined the simultaneous microanalysis of *N*-linked oligosaccharides in a glycoprotein using a microbore GCC. As models of diverse oligosaccharides, we used high-mannose-type from RNase B, sialylated complex-type from fetuin, and sialylated and desialylated fucosyl complex-type from rhEPO. These oligosaccharides were well separated by the microbore GCC in the following order: high-mannose-type, desialylated fucosyl complex-type, sialylated complex-type, and sialylated fucosyl complex-type. We also applied our method for the analysis of *N*-linked oligosaccharides in tissue plasminogen activator (t-PA), which is known to contain high-mannose-type, hybrid-type and complex-type oligosaccharides in one molecule [7–13].

2. Experimental

2.1. Materials

Fetuin and RNase B were purchased from Sigma (St. Louis, MO, USA). Peptide *N*-glycosidase-F (PNGase F) and neuraminidase (*Arthrobacter ureafaciens*) were obtained from Roche Diagnostics (Mannheim, Germany) and Nacalai Tesque, Inc. (Kyoto, Japan), respectively. The rhEPO expressed by Chinese hamster ovary (CHO) cells was epoetin β manufactured by Chugai Pharmaceutical Co., Ltd. (Tokyo, Japan). t-PA from melanoma cell lines was purchased from Biogenesis (Poole, UK). All other chemicals used were of the highest purity available.

2.2. Preparation of N-linked oligosaccharide alditols

Fetuin, RNase B, and rhEPO (400 μg) were dissolved in 400 μl of sodium phosphate buffer, pH7.2, containing 1% Triton X-100 (for fetuin and RNase B), and incubated with 10 units of PNGase F at 37 °C for 3 days (fetuin and RNase B) or for 18 h (rhEPO) [14]. Protein was precipitated with 1.36 ml of cold ethanol. The supernatant was dried, and the oligosaccharides were dissolved in 100 μl of water. To the oligosaccharide solution, 100 μl of 0.5 *M* $NaBH_4$ was added, and the mixture was incubated at 28 °C for 2 h. Diluted acetic acid (20 μl) was added to the mixture to decompose excess $NaBH_4$ and to adjust the pH to 7.0 [15]. The reaction mixture was applied to Supelclean ENVI-Carb (Supelco, Bellefonte, PA, USA) for desalting. Oligosaccharide alditols (borohydride-reduced oligosaccharides) were eluted with 30% acetonitrile containing 5 m*M* ammonium acetate. Desialylated oligosaccharide alditols were prepared from *N*-linked oligosaccharides (200 μg of rhEPO) by incubation with neuraminidase (40 m unit) in 100 m*M* ammonium acetate

buffer, pH 4.5, at 37 °C for 18 h. Lyophilized samples were dissolved in water, and aliquots were injected into the GCC-LC–MS.

2.3. Preparation of N-linked oligosaccharide alditols from t-PA

t-PA (100 μg) was dissolved in 270 μl of 0.5 *M* Tris–HCl buffer, pH 8.6, containing 8 *M* guanidine hydrochloride and 5 m*M* ethylenediaminetetraacetic acid (EDTA). After the addition of 2 μl of 2-mercaptoethanol, the mixture was allowed to stand at room temperature for 2 h. Monoiodoacetic acid (5.67 mg) was added to this solution, and the mixture was incubated at room temperature for 2 h in the dark. The reaction mixture was applied to a PD-10 column (Amersham Bioscience Corp., Piscataway, NJ, USA) to remove the reagents, and the eluate was lyophilized. Reduced and carboxymethylated t-PA (RCM-t-PA) was dissolved in 300 μl of sodium phosphate buffer, pH 7.2, containing 1% Triton X-100, and incubated with 2.5 units of PNGase F at 37 °C for 18 h. Protein was precipitated with 1020 μl of cold ethanol. The supernatant was dried, and the oligosaccharides were dissolved in 100 μl of water. To the oligosaccharide solution, 100 μl of 0.5 *M* $NaBH_4$ was added, and the mixture was incubated at room temperature for 2 h. Diluted acetic acid (20 μl) was added to the mixture to decompose excess $NaBH_4$ and to adjust the pH to 7.0. The reaction mixture was applied to Supelclean ENVI-Carb for desalting. Oligosaccharide alditols were eluted with 30% acetonitrile containing 5 m*M* ammonium acetate. Samples were dissolved in 100 μl of water, and 10-μl aliquots were injected into the microbore GCC-LC–MS.

2.4. HPLC for N-linked oligosaccharide alditols from glycoproteins

HPLC was carried out using a MAGIC 2002 system (Michrom BioResources, Auburn, CA, USA). A Hypercarb column (5 μm, 100×1.0 mm, ThermoFinnigan, San Jose, CA, USA) was used as the GCC. The eluents were 5 m*M* ammonium acetate, pH 9.6, containing 2% acetonitrile (pump A); and 5 m*M* ammonium acetate, pH 9.6, containing 80% acetonitrile (pump B). The oligosaccharide alditols were eluted at a flow-rate of 50 μl/min with a gradient of 5–40% of pump B in 80 min.

2.5. Electrospray ionization MS of oligosaccharide alditols

Mass spectra were recorded on a ThermoFinnigan TSQ 7000 triple-stage quadrupole mass spectrometer equipped with an electrospray ionization (ESI) source (ThermoFinnigan). The mass spectrometer was operated in the positive-ion mode. The mass range, m/z 700–2400, was established with a scan duration of 4 s. The ESI voltage was set at 4500 V, and the capillary temperature was 225 °C. The electron multiplier was set at 1200 V. The pressure of the sheath gas was 70 p.s.i., and that of the auxiliary gas was 10 units (1 p.s.i. = 6894.76 Pa).

3. Results

3.1. Sugar mapping by microbore GCC-LC–MS

In our previous reports, two analytical conditions were employed according to the type of oligosaccharides [5,6]. High-mannose-type oligosaccharides released from RNase B with endoglycosidase H were analyzed in the positive-ion mode using the column, 100×4.6 mm, with ammonium hydroxide as an eluent. Sialylated fucosyl complex-type oligosaccharides liberated from rhEPO with PNGase F were analyzed with in the negative-ion mode using the column, 100×2.1 mm, with ammonium acetate as a mobile phase. In this study, we used the microbore column, 100×1.0 mm for simultaneous microanalysis of oligosaccharides. Ammonium acetate was chosen as an eluent because of its higher sensitivity, and analysis in the positive-ion mode was tested for the detection of both neutral and acidic oligosaccharides. Oligosaccharides used in this study were prepared from RNase B, fetuin, and rhEPO by PNGase F treatment and reduction with $NaBH_4$ to prevent anomerization [5,15,16].

3.1.1. Analysis of high-mannose-type oligosaccharide alditols

High-mannose-type oligosaccharide alditols prepared from RNase B were analyzed by microbore

GCC-LC–MS in the positive-ion mode using ammonium acetate as an eluent (Fig. 1A). Based on our previous study, in which high-mannose-type and hybrid-type oligosaccharide alditols were eluted with acetonitrile at a low concentration [5], a gradient condition starting from 5% of pump B was used. $Man_5GlcNAc_2$ (peak A8), $Man_9GlcNAc_2$ (peak A3), isomers of $Man_6GlcNAc_2$ (peaks A1, A4, and A9), $Man_7GlcNAc_2$ (peaks A2, A4, and A5) and $Man_8GlcNAc_2$ (peaks A2, A5, and A7), and

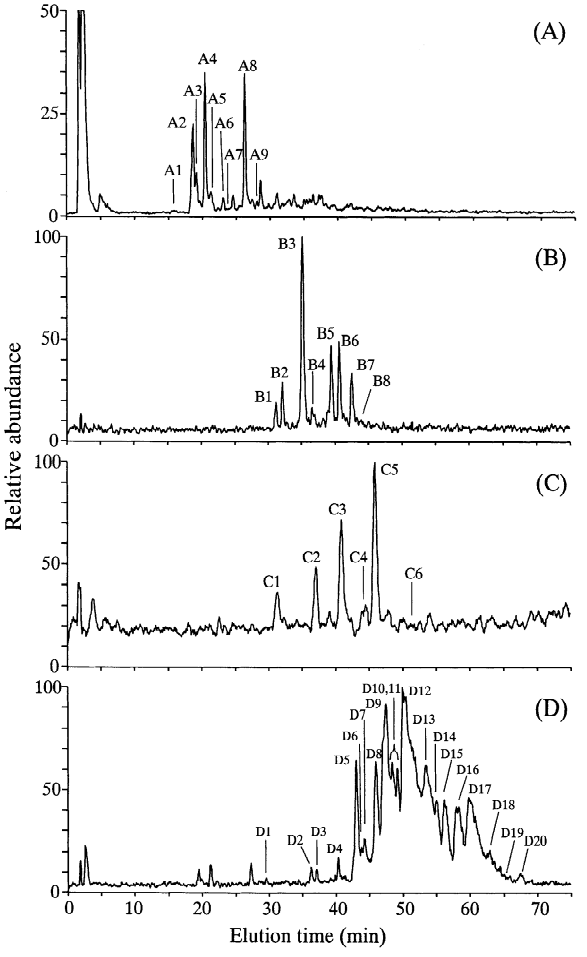

Fig. 1. TIC chromatogram of GCC-LC–MS of reduced *N*-linked oligosaccharides from RNase B (A), desialylated rhEPO (B), fetuin (C), and sialylated rhEPO (D) in the positive-ion mode. The amounts of injected oligosaccharide alditol samples were from 400 μg (A), 5 μg (B), 2 μg (C), and 2 μg (D) of glycoprotein, respectively.

Table 1
Carbohydrate structure of A1–A9 in Fig. 1A and their theoretical masses and observed *m*/*z* values

Peak no.	Carbohydrate structure[a]	Theoretical mass[b]	Observed *m*/*z*	
			M^+	M^{2+}
A1	$Man_6GlcNAc_2$	1399.3	1400.0	
A2	$Man_7GlcNAc_2$	1561.4	1562.3	782.2
	$Man_8GlcNAc_2$	1723.6	1724.4	862.8
A3	$Man_9GlcNAc_2$	1885.7	1886.9	944.2
A4	$Man_6GlcNAc_2$	1399.3	1399.8	
	$Man_7GlcNAc_2$	1561.4	1562.2	
A5	$Man_7GlcNAc_2$	1561.4	1561.1	
	$Man_8GlcNAc_2$	1723.6	1724.8	
A6	$Man_6GlcNAc_3$[c]	1602.5	1602.2	
A7	$Man_8GlcNAc_2$	1723.6	1723.9	
A8	$Man_5GlcNAc_2$	1237.1	1237.9	
A9	$Man_6GlcNAc_2$	1399.3	1399.9	

[a] Man, mannose; GlcNAc, *N*-acetylglucosamine.
[b] Average mass value.
[c] Hybrid-type.

$Man_6GlcNAc_3$ (hybrid-type, peak A6) were well separated by ammonium acetate (Table 1). The high-mannose-type oligosaccharide with greater molecular mass tended to be eluted early. Although some oligosaccharide alditols were co-eluted in this gradient condition, based on their *m*/*z* values they could be distinguished among. For example, peak A2 consists of two oligosaccharide alditols with *m*/*z* values of 1562.3 and 1724.4, and these alditols could also be characterized as $Man_7GlcNAc_2$ and $Man_8GlcNAc_2$, respectively.

3.1.2. Analysis of desialylated complex-type oligosaccharide alditols

Fig. 1B shows a total ion current (TIC) chromatogram of desialylated fucosyl complex-type oligosaccharide alditols prepared from rhEPO. Structural assignments of the peaks in Fig. 1B are summarized in Table 2. Desialylated fucosyl complex-type oligosaccharide alditols were eluted after the high-mannose-type by ammonium acetate used as an eluent. These alditols were roughly eluted in order of molecular mass; i.e., biantennary (peaks B1–6), triantennary (peaks B2–7), tetraantennary (peaks B3, B5 and B6), and tetraantennary with lactosamine repeats (peaks B5–8) (Fig. 1B, Table 2).

Table 2
Carbohydrate structure of B1–B8 in Fig. 1B and their theoretical masses and observed m/z values

Peak no.	Carbohydrate structure[a]	Theoretical mass[b]	Observed m/z		
			M^+	M^{2+}	M^{3+}
B1	FucBi	1789.7	1790.4	895.0	
B2	FucBiLac, FucTri[c]	2155.0		1078.5	
B3	FucBiLac, FucTri	2155.0	2155.8	1078.3	
	$FucBiLac_2$, FucTriLac, FucTetra[d]	2520.3		1261.0	
B4	FucBiLac, FucTri	2155.0	2154.7	1078.3	
B5	FucBiLac, FucTri	2155.0	2155.3		
	$FucBiLac_2$, FucTriLac, FucTetra	2520.3		1260.6	
	$FucTriLac_2$, FucTetraLac[e]	2885.7		1443.4	962.8
B6	FucBiLac, FucTri	2155.0	2156.1		
	$FucBiLac_2$, FucTriLac, FucTetra	2520.3		1262.2	
	$FucTriLac_2$, FucTetraLac	2885.7		1443.3	963.3
B7	$FucTriLac_2$, FucTetraLac	2885.7		1443.1	
	$FucTetraLac_2$	3251.0		1626.1	1085.2
B8	$FucTetraLac_3$	3616.4		1809.6	1206.6

[a] Fuc, fucose; Bi, biantennary; Tri, Triantennary; Tetra, tetraantennary; Lac, *N*-acetyllactosamine.
[b] Average mass value.
[c] Isomers.
[d] Isomers.
[e] Isomers.

3.1.3. Analysis of sialylated complex-type oligosaccharide alditols

Fig. 1C,D shows the TIC chromatograms of sialylated complex-type oligosaccharide alditols from fetuin and rhEPO, respectively. The carbohydrate structures of the peaks in Fig. 1C,D are summarized in Tables 3 and 4, respectively. Fucosyl tetrasialylated tetraantennary containing tri-*N*-acetyllactosamine ($FucTetraLac_3NA_4$), the largest oligosaccharide in rhEPO, was confirmed to elute by 40% of pump B (peak D20). Since the gradient condition, 5–40% of pump B in 80 min, enabled both high-mannose-type oligosaccharide alditols (hydrophilic *N*-linked oligosaccharides) and sialylated fucosyl complex-type oligosaccharide alditols (hydrophobic *N*-linked oligosaccharides) to be separated and eluted, it is reasonable to assume that most *N*-linked oligosaccharides can be analyzed under this gradient condition.

Even sialylated oligosaccharides prepared from fetuin and rhEPO could be analyzed in the positive-ion mode. In our previous study, 20 μg of rhEPO was needed in one analysis in negative-ion mode [6]. In contrast, only 2 μg of rhEPO were sufficient for analysis using the present method, in positive-ion mode. Sialylated complex-type oligosaccharide alditols are eluted after desialylated oligosaccharides; alditols prepared from rhEPO (Fig. 1D, Table 4) are eluted after desialylated oligosaccharide alditols prepared from rhEPO (Fig. 1B, Table 2). The addition of fucose on the trimannosyl core delays elution time; alditols containing fucose, prepared from

Table 3
Carbohydrate structure of C1–C6 in Fig. 1C and their theoretical masses and observed m/z values

Peak no.	Carbohydrate structure[a]	Theoretical mass[b]	Observed m/z		
			M^+	M^{2+}	M^{3+}
C1	$BiNA_2$	2226.0	2226.0	1113.7	
C2	$BiNA_2$	2226.0	2226.7	1113.9	
C3	$TriNA_3$	2882.6		1442.3	962.1
C4	$TriNA_3$	2882.6		1442.2	962.5
C5	$TriNA_3$	2882.6		1442.5	962.5
	$TriNA_2$	2591.4		1296.2	
C6	$TriNA_4$	3173.9		1587.6	1060.1

[a] Bi, biantennary; Tri, Triantennary; NA, *N*-acetylneuramic acid.
[b] Average mass value.

Table 4
Carbohydrate structure of D1–D20 in Fig. 1D and their theoretical masses and observed m/z values

Peak no.	Carbohydrate structure[a]	Theoretical mass[b]	Observed m/z		
			M^+	M^{2+}	M^{3+}
D1	FucBi	1789.7	1790.1	895.8	
D2	FucBiNA	2080.9	2081.3	1041.5	
	FucTriNA	2446.3		1223.8	
D3	FucBiNA	2080.9	2081.4	1041.6	
D4	FucTriNA	2446.3		1224.4	
	$FucBiLac_2NA$, FucTriLacNA, FucTetraNA[c]	2811.6		1406.6	
	$FucBiLac_2NA_2$, $FucTriLacNA_2$, $FucTetraNA_2$[d]	3102.9		1552.5	1035.6
D5	FucBiNA	2080.9	2081.2	1041.5	
	$FucBiNA_2$	2372.2	2372.3	1186.9	
	$FucBiLacNA_2$, $FucTriNA_2$[e]	2737.5		1369.5	
	$FucBiLac_2NA_2$, $FucTriLacNA_2$, $FucTetraNA_2$	3102.9		1552.0	
D6	FucBiNA	2080.9	2080.7	1042.9	
	$FucBiNA_2$	2372.2	2373.7	1187.1	
	$FucBiLacNA_2$, $FucTriNA_2$	2737.5		1369.7	
	$FucBiLac_2NA_2$, $FucTriLacNA_2$, $FucTetraNA_2$	3102.9		1552.2	1035.4
D7	FucBiNA	2080.9	2082.0	1040.9	
	$FucBiNA_2$	2372.2		1187.3	
	$FucBiLacNA_2$, $FucTriNA_2$	2737.5	1369.9		
	$FucBiLac_2NA_2$, $FucTriLacNA_2$, $FucTetraNA_2$	3102.9		1551.8	1035.8
	$FucTriLac_2NA_2$, $FucTetraLacNA_2$[f]	3468.2		1735.0	1157.4
D8	FucBiNA	2080.9	2081.4	1041.3	
	$FucBiLacNA_2$, $FucTriNA_2$	2737.5		1369.6	
	$FucBiLac_2NA_2$, $FucTriLacNA_2$, $FucTetraNA_2$	3102.9		1553.1	
	$FucTriLacNA_3$, $FucTetraNA_3$[g]	3394.1		1698.1	1132.3
D9	$FucBiNA_2$	2372.2	2373.1		
	$FucBiLacNA_2$, $FucTriNA_2$	2737.5		1370.2	
	$FucTriNA_3$	3028.8		1515.5	1011.1
	$FucBiLac_2NA_2$, $FucTriLacNA_2$, $FucTetraNA_2$	3102.9		1552.3	
	$FucTriLacNA_3$, $FucTetraNA_3$	3394.1		1698.0	1132.9
	$FucTriLac_2NA_3$, $FucTetraLacNA_3$[h]	3759.5		1881.0	1254.5
D10	$FucBiNA_2$	2372.2	2372.4		
	$FucBiLacNA_2$, $FucTriNA_2$	2737.5		1370.3	
	$FucTriNA_3$	3028.8		1515.4	
	$FucBiLac_2NA_2$, $FucTriLacNA_2$, $FucTetraNA_2$	3102.9		1552.6	
	$FucTriLacNA_3$, $FucTetraNA_3$	3394.1		1698.3	1132.4
	$FucTriLac_2NA_3$, $FucTetraLacNA_3$	3759.5		1880.0	1254.1
D11	$FucBiNA_2$	2372.2	2373.3		
	$FucBiLacNA_2$, $FucTriNA_2$	2737.5		1370.0	
	$FucTriNA_3$	3028.8		1516.2	
	$FucBiLac_2NA_2$, $FucTriLacNA_2$, $FucTetraNA_2$	3102.9		1552.0	
	$FucTriLacNA_3$, $FucTetraNA_3$	3394.1		1697.5	1132.5
	$FucTriLac_2NA_3$, $FucTetraLacNA_3$	3759.5		1880.5	1254.1
D12	$FucBiNA_2$	2372.2	2372.5		
	$FucBiLacNA_2$, $FucTriNA_2$	2737.5		1369.7	
	$FucTriNA_3$	3028.8		1515.5	
	$FucBiLac_2NA_2$, $FucTriLacNA_2$, $FucTetraNA_2$	3102.9		1553.3	
	$FucTriLacNA_3$, $FucTetraNA_3$	3394.1		1697.8	1132.4
	$FucTetraNA_4$	3685.4		1843.4	1229.5
	$FucTetraLac_2NA_3$	4124.8		2062.9	1376.0

Table 4. Continued
Carbohydrate structure of D1–D20 in Fig. 1D and their theoretical masses and observed m/z values

Peak no.	Carbohydrate structure[a]	Theoretical mass[b]	Observed m/z		
			M^{+}	M^{2+}	M^{3+}
D13	$FucTriNA_3$	3028.8		1515.0	
	$FucBiLac_2NA_2$, $FucTriLacNA_2$, $FucTetraNA_2$	3102.9		1552.6	
	$FucTriLacNA_3$, $FucTetraNA_3$	3394.1		1698.2	1132.8
	$FucTetraNA_4$	3685.4		1843.5	1229.4
	$FucTetraLacNA_4$	4050.7		2026.0	1351.1
	$FucTetraLac_2NA_3$	4124.8		2063.5	1375.9
D14	$FucTriNA_3$	3028.8		1515.4	
	$FucBiLac_2NA_2$, $FucTriLacNA_2$, $FucTetraNA_2$	3102.9		1552.6	
	$FucTriLacNA_3$, $FucTetraNA_3$	3394.1		1697.8	
	$FucTetraNA_4$	3685.4		1842.8	1229.1
	$FucTriLac_2NA_3$, $FucTetraLacNA_3$	3759.5		1880.1	1254.1
	$FucTetraLacNA_4$	4050.7		2026.5	1351.7
	$FucTetraLac_2NA_3$	4124.8		2062.8	1375.9
	$FucTetraLac_3NA_3$	4490.1			1497.5
D15	$FucBiLac_2NA_2$, $FucTriLacNA_2$, $FucTetraNA_2$	3102.9		1552.5	
	$FucTriLacNA_3$, $FucTetraNA_3$	3394.1		1697.7	1132.2
	$FucTriLac_2NA_2$, $FucTetraLacNA_2$	3468.2		1735.9	1157.0
	$FucTetraNA_4$	3685.4		1842.6	1229.4
	$FucTriLac_2NA_3$, $FucTetraLacNA_3$	3759.5		1880.7	1254.0
	$FucTetraLac_2NA_3$	4124.8		2062.7	1376.4
	$FucTetraLac_3NA_3$	4490.1		2246.4	1498.1
D16	$FucTriLacNA_3$, $FucTetraNA_3$	3394.1		1697.8	1133.1
	$FucTriLac_2NA_2$, $FucTetraLacNA_2$	3468.2		1735.2	
	$FucTriLac_2NA_3$, $FucTetraLacNA_3$	3759.5		1879.8	1254.3
	$FucTetraLacNA_4$	4050.7		2026.5	1351.4
	$FucTetraLac_2NA_3$	4124.8			1375.8
	$FucTetraLac_2NA_4$	4416.1		2208.9	1472.9
D17	$FucBiLac_2NA_2$, $FucTriLacNA_2$, $FucTetraNA_2$	3102.9		1553.0	
	$FucTriLacNA_3$, $FucTetraNA_3$	3394.1		1697.7	
	$FucTriLac_2NA_3$, $FucTetraLacNA_3$	3759.5		1880.8	1254.3
	$FucTetraLacNA_4$	4050.7		2026.1	1351.2
	$FucTetraLac_2NA_4$	4416.1		2208.7	1473.4
	$FucTetraLac_3NA_4$	4781.4			1594.4
D18	$FucTriLacNA_3$, $FucTetraNA_3$	3394.1		1697.8	
	$FucTriLac_2NA_3$, $FucTetraLacNA_3$	3759.5		1881.6	
	$FucTetraLacNA_4$	4050.7		2025.5	1351.8
	$FucTetraLac_2NA_4$	4416.1		2208.3	1473.1
	$FucTetraLac_3NA_4$	4781.4			1594.9
D19	$FucTriLacNA_3$, $FucTetraNA_3$	3394.1		1696.7	
	$FucTriLac_2NA_3$, $FucTetraLacNA_3$	3759.5		1880.7	
	$FucTetraLacNA_4$	4050.7		2025.5	1350.4
	$FucTetraLac_3NA_4$	4781.4			1595.6
D20	$FucTriLac_2NA_3$, $FucTetraLacNA_3$	3759.5		1880.0	
	$FucTetraLac_3NA_4$	4781.4			1595.0

[a] Fuc, fucose; Bi, biantennary; Tri, Triantennary; Tetra, tetraantennary; NA, *N*-acetylneuramic acid; Lac, *N*-acetyllactosamine.
[b] Average mass value.
[c] Isomers.
[d] Isomers.
[e] Isomers.
[f] Isomers.
[g] Isomers.
[h] Isomers.

rhEPO (Fig. 1D, Table 4), are eluted later than those without fucose, prepared from fetuin (Fig. 1C, Table 3).

3.2. Application of sugar mapping by GCC-LC–MS to t-PA

Microbore GCC-LC–MS successfully analyzed model oligosaccharide alditols simultaneously under the established analytical conditions. We then applied our method to the analysis of *N*-linked oligosaccharides in t-PA produced from human melanoma cells. *N*-linked oligosaccharides were released from RCM-t-PA by digestion with PNGase F, and their alditols were subjected to microbore GCC-LC–MS under the established conditions. Fig. 2 shows the TIC chromatogram of microbore GCC-LC–MS of *N*-linked oligosaccharide alditols from t-PA. We can estimate what types of oligosaccharides are attached to t-PA primarily on the basis of the elution time of the major peaks in Fig. 2. It is predicted that the major peaks a, c, h, and k are $Man_6GlcNAc_2$ and/or $Man_7GlcNAc_2$, $Man_5GlcNAc_2$, fucosyl monosialylated biantennary (FucBiNA), and fucosyl disialylated biantennary ($FucBiNA_2$), respectively. These structures can be confirmed on the basis of the m/z values in mass spectra. Fig. 3 is a two-dimensional display (elution time versus m/z value) of the sugar map by GCC-LC–MS. Ions are visually displayed based on their m/z values and elution time, and the minor oligosaccharides that were co-eluted with major ones and which appear as small peaks in Fig. 2 can be characterized by a two-dimensional display. For example, peak h is a single peak on a TIC chromatogram, however, the two-dimensional

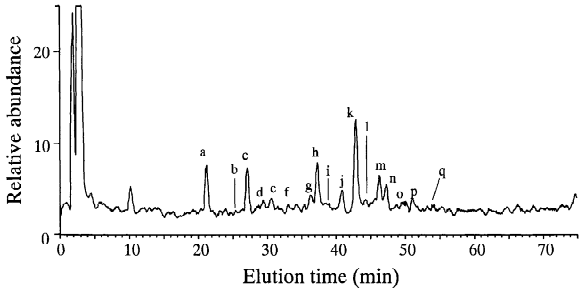

Fig. 2. TIC chromatogram of GCC-LC–MS of *N*-linked oligosaccharide alditols from 10 μg of t-PA in the positive-ion mode.

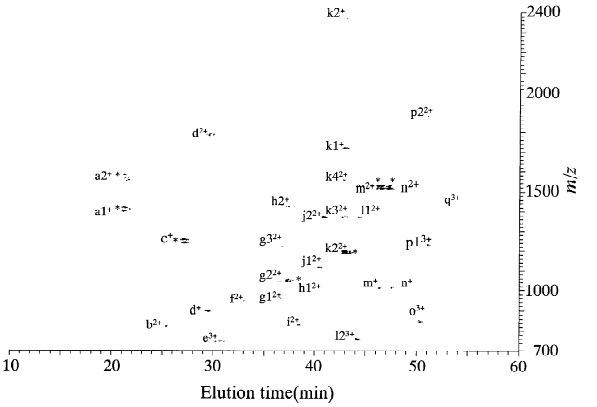

Fig. 3. Two-dimensional display of the TIC of *N*-linked oligosaccharide alditols from t-PA. *Ammonium adduct of oligosaccharide alditol.

display clearly shows that it is composed of not only FucBiNA but also co-eluted FucBi(1) (h1 and h2 in Table 5, respectively). Likewise, minor peaks can be determined to be hybrid-type, complex-type without fucose, and/or galactose and complex-type not with *N*-acetyllactosamine but with GalNAc–GlcNAc moiety (see b, f, i, l, o, and q in Fig. 3 and Table 5).

The resulting structural assignments of the peaks shown in Figs. 2 and 3 are summarized in Table 5, and the deduced carbohydrate structures are listed in Table 6. The *N*-linked oligosaccharides in t-PA are mainly high-mannose-type ($Man_6GlcNAc_2$ and $Man_5GlcNAc_2$) and complex-type (fucosylated biantennary and triantennary). Most hybrid-type and complex-type oligosaccharides are sialylated, and the heterogeneity of *N*-acetylneuramic acid linking to them can be observed.

In the positive-ion mode, the sensitivity of neutral and acidic oligosaccharide alditols may be approximately equivalent. Therefore, the height of the peaks in Fig. 2 roughly represents the ratio of oligosaccharide contents and contributes to an understanding of the distribution of carbohydrates and their heterogeneity. In cases in which a single peak consists of several oligosaccharide alditols, the peak height shows their sum. The ratio of oligosaccharide alditols in a single peak is confirmed by further comparing their signal height on mass spectra. For instance, almost identical amounts of $Man_6GlcNAc_2$ and/or $Man_7GlcNAc_2$ and $Man_5GlcNAc_2$ are contained in t-PA based on the fact that peak a is as high

Table 5
Carbohydrate structure of peak a–q in Figs. 2 and 3 and their theoretical masses and observed m/z values

Peak no. in Fig. 2	Peak no. in Fig. 3	Carbohydrate composition[a]	Sugar type[b]	Theoretical mass[c]	Observed m/z		
					M^+	M^{2+}	M^{3+}
a	a1	$[Hex]_6[HexNAc]_2$	M6	1399.3	1399.6		
	a2	$[Hex]_7[HexNAc]_2$	M7	1561.4	1562.2		
b	b	$[Hex]_5[HexNAc]_4$	Bi, Hybrid(2)	1643.5		822.9	
c	c	$[Hex]_5[HexNAc]_2$	M5	1237.1	1237.5		
d	d	$[Fuc][Hex]_5[HexNAc]_4$	FBi	1789.7	1789.3	895.6	
e	e	$[Fuc][Hex]_4[HexNAc]_7$	FTri(3)	2237.1			747.3
f	f	$[Hex]_6[HexNAc]_3[NeuAc]$	Hybrid(1)NA	1893.7		948.1	
g	g1	$[Fuc][Hex]_4[HexNAc]_4[NeuAc]$	FBi(3)NA	1918.8		960.3	
	g2	$[Fuc][Hex]_5[HexNAc]_4[NeuAc]$	FBiNA	2080.9		1041.1	
	g3	$[Fuc][Hex]_6[HexNAc]_5[NeuAc]$	FTriNA	2446.3		1224.7	
h	h1	$[Fuc][Hex]_5[HexNAc]_4[NeuAc]$	FBiNA	2080.9		1041.2	
	h2	$[Fuc][Hex]_4[HexNAc]_3$	FBi(1)	1424.3	1424.5		
i	i	$[Fuc][Hex]_3[HexNAc]_5$	FTri(1), FBi(4)	1668.6		835.6	
j	j1	$[Hex]_5[HexNAc]_4[NeuAc]_2$	$BiNA_2$	2226.0		1113.9	
	j2	$[Fuc][Hex]_6[HexNAc]_5[NeuAc]_2$	$FTriNA_2$	2737.5		1369.4	
k	k1	$[Fuc][Hex]_4[HexNAc]_3[NeuAc]$	FBi(1)NA	1715.6	1717.1		
	k2	$[Fuc][Hex]_5[HexNAc]_4[NeuAc]_2$	$FBiNA_2$	2372.2	2373.1	1186.7	
	k3	$[Fuc][Hex]_6[HexNAc]_5[NeuAc]_2$	$FTriNA_2$	2737.5		1369.9	
	k4[d]	$[Fuc][Hex]_7[HexNAc]_6[NeuAc]_2$	$FTetraNA_2$	3102.9		1553.0	
	k4[d]	$[Hex]_9[HexNAc]_8[NeuAc]_2$	$TetraLac_2$	3104.9		1553.0	
l	l1	$[Fuc][Hex]_6[HexNAc]_5[NeuAc]_2$	$FTriNA_2$	2737.5		1369.5	
	l2	$[Hex]_4[HexNAc]_5[NeuAc]_2$	$Tri(1)NA_2$, $Bi(1)NA_2$	2267.1			756.6
m	m	$[Fuc][Hex]_6[HexNAc]_5[NeuAc]_3$	$FTriNA_3$	3028.8		1515.4	1011.1
n	n	$[Fuc][Hex]_6[HexNAc]_5[NeuAc]_3$	$FTriNA_3$	3028.8		1514.7	1010.6
o	o	$[Fuc][Hex]_4[HexNAc]_7[NeuAc]$	FTri(3)NA	2528.4			844.7
p	p1[d]	$[Fuc][Hex]_7[HexNAc]_6[NeuAc]_4$	$FTetraNA_4$	3685.4			1229.5
	p1[d]	$[Hex]_9[HexNAc]_8[NeuAc]_2$	$BiLac_4NA_2$, $TriLac_3NA_2$, $TetraLac_2NA_2$	3687.4			1229.5
	p2[d]	$[Fuc][Hex]_8[HexNAc]_7[NeuAc]_3$	$FBiLac_3NA_3$, $FTriLac_2NA_3$, $FTetraLacNA_3$	3759.5		1880.9	
	p2[d]	$[Hex]_{10}[HexNAc]_9[NeuAc]$	$TetraLac_3NA$	3761.5		1880.9	
q	q	$[Fuc][Hex]_5[HexNAc]_5[NeuAc]_3$	$FTri(2)NA_3$	2866.6		1434.4	

[a] Hex, hexose; Fuc, fucose; HexNAc, *N*-acetylhexosamine; NeuAc, *N*-acetylneuramic acid.
[b] See Table 6, except the following; F, fucose; NA, *N*-acetylneuramic acid; Lac, *N*-acetyllactosamine.
[c] Average mass value.
[d] Glycoforms are not distinguishable by m/z value.

as peak c in Fig. 2. Peak a shows a higher amount of $Man_6GlcNAc_2$ than of $Man_7GlcNAc_2$ on the basis of their respective signal heights on mass spectra (data not shown). The distribution of carbohydrates can also be analyzed by peak height.

4. Discussion

We explored the expansion of GCC-LC–MS for the use in the simultaneous microanalysis of *N*-linked oligosaccharides from glycoprotein. The models used in this study were RNase B, fetuin, and rhEPO. RNase B has a single *N*-glycosylation site containing high-mannose-type oligosaccharides ranging from $Man_5GlcNAc_2$ to $Man_9GlcNAc_2$ as well as a hybrid-type oligosaccharide, $Man_6GlcNAc_3$ [5,17–19]. Each $Man_{6-8}GlcNAc_2$ has three positional isomers [5]. rhEPO has three *N*-glycosylation sites containing sialylated fucosyl biantennary, triantennary, and tetraantennary oligosaccharides with or without *N*-acetyllactosamine repeats. Desialylated fucosyl complex-type *N*-linked oligosaccharides were prepared from rhEPO by treatment with neuraminidase. Fetuin has three *N*-glycosylation sites

Table 6
Structure and theoretical mass of *N*-linked oligosaccharide alditols in Table 5

Abbreviation	Structure[a]	Theoretical mass[b]
M5	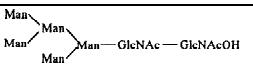	1237.1
M6	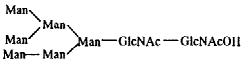	1399.3
M7	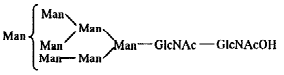	1561.4
Hybrid(1)	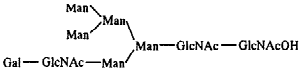	1602.5
Hybrid(2)	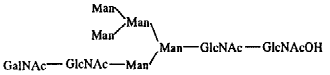	1643.5
Bi	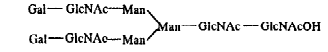	1643.5
Bi(1)	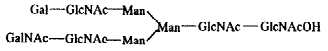	1684.6
FBi	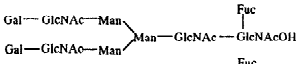	1789.7
FBi(1)	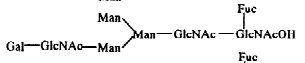	1424.3
FBi(2)	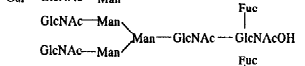	1465.4
FBi(3)	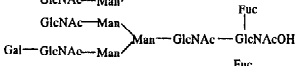	1627.5
FBi(4)	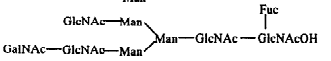	1668.6
Tri	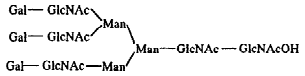	2008.9
Tri(1)	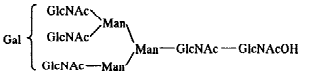	1684.6
FTri	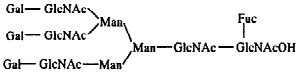	2155.0
FTri(1)	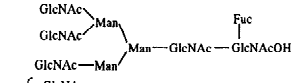	1668.6
FTri(2)	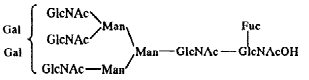	1992.9
FTri(3)	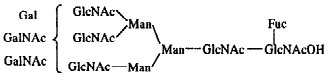	2237.1
Tetra	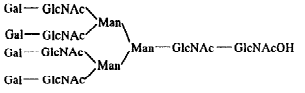	2374.2
FTetra	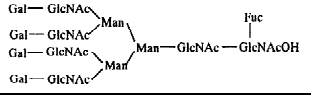	2520.3

[a] Man, mannose; Fuc, fucose; Gal, galactose; GalNAc, *N*-acetylgalactosamine; GlcNAc, *N*-acetylglucosamine. The structure are based upon the known structure of t-PA (10, 11, 12). [b] Average mass value.

containing bi-, tri-, and tetrasialylated bi- and triantennary oligosaccharides without fucose linked to the trimannosyl core [20].

In this study, microbore GCC-LC–MS was successful in the separation of various *N*-linked oligosaccharides in a single analysis. The oligosaccharides were eluted as follows: (i) *N*-linked oligosaccharide, in order of high-mannose-type and complex-type, desialylated, and sialylated; (ii) high-mannose-type oligosaccharide alditols, in descending order of molecular mass, while the complex-type was eluted in ascending order of molecular mass; (iii) elution time of complex-type oligosaccharide alditols was prolonged by the addition of fucose on the trimannosyl core; and (iv) sialylation delayed the elution of oligosaccharide alditols. Namely, we confirmed that this methods was able to elucidate the structure of diverse *N*-linked oligosaccharides in a single analysis.

Repeated analysis ($n=3$) showed that high-mannose-type, $Man_5GlcNAc_2$, and complex-type, fucosyl disialylated bianntenary ($FucBiNA_2$), are eluted at an average of 27.2 min and 43.9 min, with relative standard deviations of 0.7 and 1.9%, respectively (data not shown). Reproducibility of the elution time under the employed condition was acceptable for the analysis. Therefore, on the basis of elution times in the sugar map, the types of oligosaccharide (high-mannose-, hybrid-, and complex-type) contained in a given glycoprotein can be roughly estimated. This facilitates the assignment of the peaks in the sugar map. Additionally, it is possible to estimate the structure of positional isomers by comparing their elution times with those of established standards.

Other methods in which HPLC is used for separation of derivatized oligosaccharides (such as 2-AP and 2-AB derivatives) require combining several types of column. Our method enabled us to separate various types of *N*-linked oligosaccharides, including high-mannose-type and complex-type (sialylated or not), with one GCC in a single analysis. Furthermore, our method does not require complicated steps for derivatization.

By use of the microbore column, we succeeded not only in performing simultaneous analysis of *N*-linked oligosaccharides, but also in improving the sensitivity on LC–MS. There have been several studies on the sensitivity of derivatized glycans in MS by different ionization methods, including ESI, fast atom bombardment (FAB), and matrix-assisted laser desorption ionization (MALDI), under different conditions [21–27]. In these studies, sensitivity of oligosaccharides was enhanced by derivatization with a volatile compound and compounds that have high-proton-affinity or positively charged site. Likewise, we found that derivatization with 2-AP is more effective for the sensitive analysis of oligosaccharides by LC–ESI-MS. The details of those results will be reported elsewhere.

Using our methods, we analyzed the structure of *N*-linked oligosaccharides in t-PA. t-PA is composed of 527 amino acid residues and has three *N*-linked glycosylation sites. It has been reported that high-mannose-type oligosaccharides are attached to Asn-117, while complex-type oligosaccharides are linked to Asn-184 and -448, either or both [7–12]. The carbohydrate structures in t-PA have been previously characterized by use of a combination of several methods; specifically, by methylation analysis including FAB-MS, MALDI time-of-flight MS (MALDI-TOF-MS), NMR, high-pH anion-exchange chromatography with pulsed amperometric detection (HPAEC–PAD), and serial chromatographies after sequential exoglycosidase digestions of radiolabeled oligosaccharide alditols [8–13]. These methods required a large amount of the sample and are time consuming due to the many complicated steps required to perform for analysis. We have demonstrated that microbore GCC-LC–MS is able to elucidate the structure of *N*-linked oligosaccharides in t-PA in a single analysis, requiring no complicated steps. *N*-linked oligosaccharides in t-PA are confirmed to be primarily of the high-mannose-type ($Hex_6HexNAc_2$ and $Hex_5HexNAc_2$) and of the complex-type (fucosyl biantennary and triantennary).

We successfully conducted the simultaneous microanalysis using microbore GCC-LC–MS, and demonstrated its usefulness for the structural analysis of *N*-linked oligosaccharides in glycoproteins. This method has been shown to be useful and appropriate for the detailed examination of carbohydrate distribution, content, and heterogeneity, that is, for sensitive profiling of the oligosaccharides in glycoproteins, and is also appropriate for studying glycoproteins in a biological sample.

References

[1] A. Varki, Glycobiology 3 (1993) 97.
[2] J.C. Bigge, T.P. Patel, J.A. Bruce, P.N. Goulding, S.M. Charles, R.B. Parekh, Anal. Biochem. 230 (1995) 229.
[3] S. Hase, T. Ikenaka, Y. Matsushima, Biochem. Biophys. Res. Commun. 85 (1978) 257.
[4] S. Hase, S. Natsuka, H. Oku, T. Ikenaka, Anal. Biochem. 167 (1987) 321.
[5] N. Kawasaki, M. Ohta, S. Hyuga, O. Hashimoto, T. Hayakawa, Anal. Biochem. 269 (1999) 297.
[6] N. Kawasaki, M. Ohta, S. Hyuga, M. Hyuga, T. Hayakawa, Anal. Biochem. 285 (2000) 82.
[7] G. Pohl, L. Kenne, B. Nilsson, M. Einarsson, Eur. J. Biochem. 170 (1987) 69.
[8] M.W. Spellman, L.J. Basa, C.K. Leonard, J.A. Chakel, J.V. O'Connor, S. Wilson, H. van Halbeek, J. Biol. Chem. 264 (1989) 14100.
[9] R.B. Parekh, R.A. Dwek, P.M. Rudd, J.R. Thomas, T.W. Rademacher, T. Warren, T.C. Wun, B. Hebert, B. Reitz, M. Palmier, T. Ramabhadrm, D.C. Tiemeier, Biochemistry 28 (1989) 7670.
[10] R.B. Parekh, R.A. Dwek, J.R. Thomas, G. Opdenakker, T.W. Rademacher, A.J. Wittwer, S.C. Howard, R. Nelson, N.R. Siegel, M.G. Jennings, N.K. Harakas, J. Feder, Biochemistry 28 (1989) 7644.
[11] A.J. Jaques, G. Opdenakker, T.W. Rademacher, R.A. Dwek, S.E. Zamze, Biochem. J. 316 (1996) 427.
[12] A.L. Chan, H.R. Morris, M. Panico, A.T. Etienne, M.E. Rogers, P. Gaffney, L. Creighton-Kempsford, A. Dell, Glycobiology 1 (1991) 173.
[13] D.I. Papac, J.B. Briggs, E.T. Chin, A.J. Jones, Glycobiology 8 (1998) 445.
[14] T.H. Plummer Jr., J.H. Elder, S. Alexander, A.W. Phelan, A.L. Tarentino, J. Biol. Chem. 259 (1984) 10700.
[15] P.H. Lipniunas, D.C. Neville, R.B. Trimble, R.R. Townsend, Anal. Biochem. 243 (1996) 203.
[16] J.Q. Fan, A. Kondo, I. Kato, Y.C. Lee, Anal. Biochem. 219 (1994) 224.
[17] C.-J. Liang, K. Yamashita, A. Kobata, J. Biochem. 88 (1980) 51.
[18] A. Guttman, T. Pritchett, Electrophoresis 16 (1995) 1906.
[19] D. Fu, L. Chen, R.A. O'Neill, Carbohydr. Res. 261 (1994) 173.
[20] E.D. Green, G. Adelt, J.U. Baenziger, S. Wilson, H. Van Halbeek, J. Biol. Chem. 263 (1988) 18253.
[21] M. Okamoto, Biosci. Biotechnol. Biochem. 65 (2001) 2519.
[22] X. Shen, H. Perreault, J. Mass. Spectrom. 34 (1999) 502.
[23] K. Yoshino, T. Takao, H. Murata, Y. Shimonishi, Anal. Chem. 67 (1995) 4028.
[24] S. Suzuki, K. Kakehi, S. Honda, Anal. Chem. 68 (1996) 2073.
[25] W. Mo, T. Takao, H. Sakamoto, Y. Shimonishi, Anal. Chem. 70 (1998) 4520.
[26] N. Viseux, X. Hronowski, J. Delaney, B. Domon, Anal. Chem. 73 (2001) 4755.
[27] J. Gu, T. Hiraga, Y. Wada, Biol. Mass. Spectrom. 23 (1994) 212.